Electromagnetic Field Analyses of REBCO Roebel Cables Wound into Coil Configurations

Yusuke Sogabe, Masahiro Nii, Tadaaki Tsukamoto, Taketsune Nakamura, Naoyuki Amemiya

Abstract—We have been developing a model for numerical electromagnetic field analyses of REBCO Roebel cables wound into coil configurations, considering their three-dimensional structure. Electromagnetic field analyses were carried out for one-turn circular closed-loop of a Roebel cable, one turn circular closed-loop of a Roebel cable at the end of a stack of Roebel-cable loops which simulated a solenoid coil of a finite length, and an infinite solenoid coil wound with a Roebel cable. From the temporal evolution of the current distribution in the Roebel cables, ac losses were calculated. We studied the ac loss characteristics of Roebel cables in different locations in coils. The influence of the gap between turns on ac losses was discussed.
1

Index Terms—Ac loss, Coated conductor, Coil, Electromagnetic field analyses, Roebel cable.

I. INTRODUCTION

As one of the large-current conductor consisting of REBCO coated conductors, Roebel cable has been attracting broad interest [1]. Ac loss characteristics of straight Roebel cables have been studied by various authors [2]-[9], but there are few reports on experiments and calculations of ac losses in coils wound with Roebel cables [10], [11].

In this study, we developed a model for numerical electromagnetic field analyses of a coil wound with a Roebel cable (Roebel coil) and applied this model to Roebel cables in various coils. Then, we calculated the ac loss from the temporal development of field distribution in the superconductor of the Roebel coils. We focused on the ac loss characteristics of Roebel cables in different locations in a coil and gaps between turns (turn gap) in coils.

II. MATHEMATICAL MODELING OF COIL WOUND WITH ROEBEL CABLE

From Faraday's law and the thin-strip approximation, the governing equation of the electromagnetic field in a coated conductor with three-dimensional shape composing Roebel cables can be given as [12]

$$\nabla \times \left(\frac{1}{\sigma} \nabla \times \boldsymbol{n}T \right) \cdot \boldsymbol{n}$$
$$+ \frac{\partial}{\partial t} \left(\frac{\mu_0 t_s}{4\pi} \int_{S'} \frac{(\nabla \times \boldsymbol{n}'T') \times \boldsymbol{r} \cdot \boldsymbol{n}}{r^3} dS' + \boldsymbol{B}_{\text{ext}} \cdot \boldsymbol{n} \right) = 0 \quad , \quad (1)$$
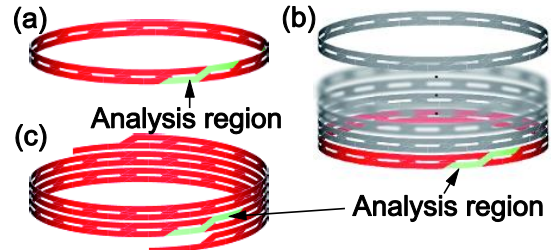
Fig. 1. The shape of the coils: (a) Model I; (b) Model E; (c) Model M.

where T and T' are the magnitudes of the current vector potentials at the field point and the source point, respectively. The superconducting property is given by the equivalent conductivity σ obtained from the power law E–J characteristic,

$$\sigma = J_c / E_0 \left(J_c / J \right)^{n-1} , \quad (2)$$

where J_c is the critical current density and E_0 is defined electric field. J_c of each element depends on the magnetic field as follows [13]:

$$J_c(B_n) = J_{c0} \frac{B_0}{B_0 + |B_n|} , \quad (3)$$

where B_0 is a constant, B_n is the local magnetic flux density normal to each element, and J_{c0} is the critical current density when $B_n = 0$, respectively.

We built three models for Roebel coils as follows: Model I for the isolated one-turn circular closed-loop of a Roebel cable, Model E for the one-turn circular closed-loop of a Roebel cable at the end of a stack of Roebel cable loops, and Model M for the one-turn of a Roebel cable wound into an infinite solenoid coil. These models are shown in Fig. 1.

A straight Roebel cable has a periodic structure: a geometry shown in Fig. 2 appears repeatedly. When we built the models for Roebel coils, we basically used similar periodic structure. We extended the model for a straight Roebel cable to the model for the Roebel coil consisting of a curved Roebel cable.

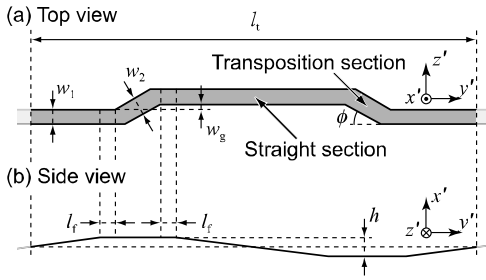The central angle of the coil shown in Fig. 3 is defined as follows:

Fig. 2.   Geometry of a strand in a Roebel cable and parameters that define the shape of strand.

$$\theta = \frac{2\pi y'}{\sqrt{(2\pi R)^2 + (w_s + w_{tg})^2}}, \qquad (4)$$

where y' is the y-coordinate of point P′ in the original straight Roebel cable shown in Fig. 3(a), R is the radius of the coil measured from the center of the coil to the center line of the Roebel cable, w_s is $2w_1 + w_g$ and w_{tg} is the turn gap, respectively. When apply this model to one-turn circular closed-loop (Models I and E), we assume that $w_s + w_{tg}$ is zero in (4)-(6). Using θ, we can derive the coordinates (x, y, z) of point P in the Roebel coil shown in Fig. 3(b) from the coordinates (x', y', z') of straight Roebel cable shown in Fig. 3(a) as follows:

$$x = (R + x')\cos\theta,$$
$$y = (R + x')\sin\theta, \qquad (5)$$
$$z = z' + \frac{\theta}{2\pi}(w_s + w_{tg}),$$

The angle ψ is introduced to represent the periodic structure in the coil.

$$\psi = \frac{2\pi l_t / n_s}{\sqrt{(2\pi R)^2 + (w_s + w_{tg})^2}} \qquad (6)$$

where, l_t is the transposition length of strand in Fig. 2, and n_s is the number of strands. In Model M, we can express the periodic structure of Roebel coil by the points P_m shifted point P in the Roebel coils. These points' coordinates are derived by using ψ as follows:

$$x_m = x\cos m\phi - y\sin m\phi,$$
$$y_m = x\sin m\phi + y\cos m\phi, \qquad (7)$$
$$z_m = z + \frac{m\phi}{2\pi}(w_s + w_{tg}),$$

where m is an integer. In the Models E and I, we have to change the expression of z_m to

$$z_m = z + \left\lfloor m \middle/ \frac{2\pi R}{l_t / n_s} \right\rfloor (w_s + w_{tg}). \qquad (8)$$
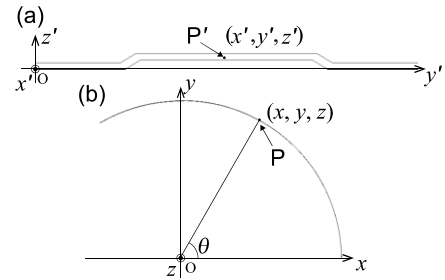

Fig. 3.   The coordinates in the strand; (a) Roebel cable, (b) Roebel coil.

On the one-turn closed-loop, $2\pi R$ is the multiple of l_t. m is a positive integer in Model E or zero in Model I. The center line of the Roebel cable in Model M is given using the real number α as follows:

$$x = r\cos\alpha,$$
$$y = r\sin\alpha, \qquad (9)$$
$$z = \frac{(w_s + w_{tg})\alpha}{2\pi}.$$

III.   RESULTS AND DISCUSSION

A.   Specifications of Superconductors and Coils

A strand of Roebel cable has zigzag shape as shown in Fig. 2. We assumed the parameters that define the shape of strands of the Roebel cable as follows: $l_t = 300$ mm, $l_f = w_1 = 5$ mm, $w_2 = 6$ mm, $w_g = 2$ mm, $\theta = 30$ degrees, and $h = 0.65$ mm. The Roebel cables consisted of six strands, its critical current density J_{c0}, was 4.0×10^{10} A·m^{-2}. The constant of t_s, E_0 and B_0 in (1)-(3) were 1 μm, 10^{-4} V·m^{-1} and 50.0×10^{-3} T, respectively. The diameters of the Roebel coils were about 0.3 m, and the height of the Roebel coil in Model E was 450 mm. We changed the turn gap of the coils in Models E and M to study its influence on ac loss characteristics.

B.   Ac Loss in Strand of the Roebel Coil

We calculated the ac loss in one turn of the Roebel cable for the three models. Before the calculations of ac loss, we determined the critical current I_c in all cases by following method: in our models, we applied current and ramped up gradually as we could ignore the effect of electromagnetic induction for all, and we determined I_c as the transport current when the electric field E reached E_0. The reference I_c was 185 A, this calculation condition was the isolated strand of straight Roebel cable. The frequency of the coil current was 50 Hz, and the current load ratio I_t / I_c was 0.3 and 0.7, respectively. When we calculated ac loss, the models were sectioned into triangular meshes. The number of meshes of analysis region was equal for all cases, 32,160. On the other hand, the computing time was different in all cases, but for same current load ratio, the computing time was nearly equal; the average computing time was 29 and 144 hours when I_t / I_c was 0.3 and 0.7, respectively (used CPU is Intel® Xeon® W5590, 3.33GHz).

The ac losses in the three models are compared in Fig. 4. First, comparing Model E with Model M, the ac losses in Model M, which simulates the middle of coils, are less than those in Model E, which simulates the ends of coils. This is because that
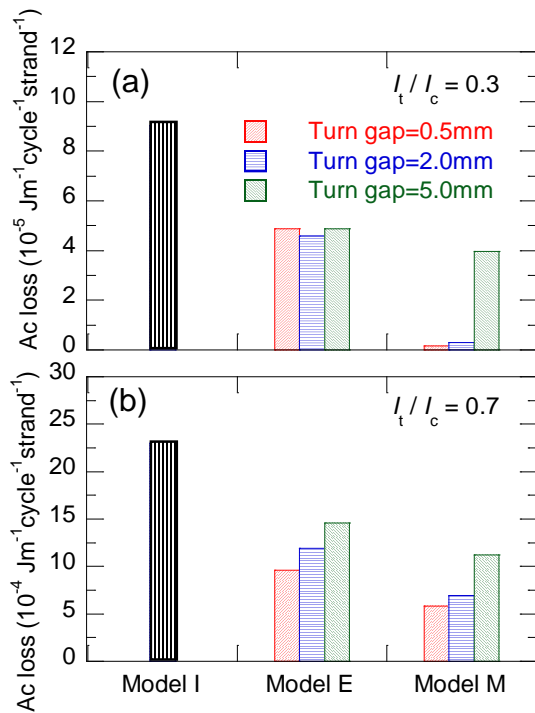
Fig. 4. Ac loss of the entire coil: (a) $I_t / I_c = 0.3$, (b) $I_t / I_c = 0.7$.
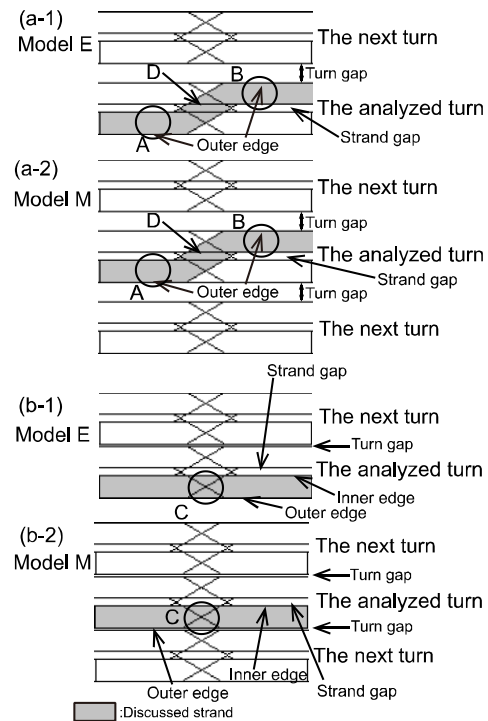

Fig. 5. The adjoining with next turn in the coil: (a) is the case turn gap is 5.0 mm, (b) is the case turn gap is 0.5 mm: (a-1) and (b-1) Model E, (a-2) and (b-2) Model M.

the magnetic field produced by the coil current bends outward at the coil ends, and the magnetic field component normal to the wide face of coated conductor (normal magnetic field component) appears at the coil ends.

Second, we look at the influence of turn gaps. Except the Model E at $I_t / I_c = 0.3$, with decreasing turn gap, the ac loss decreases. When turn gap is small, the normal magnetic field component at the edge is well canceled by the adjoining turns: the local distortion of magnetic field at turn gaps is small (*the canceling effect*). With smaller turn gap, the magnetic field generated by other turns becomes large because the number of turns of coil becomes large, in consequence, the generation of ac loss can be large (*the other turns effect*). In the results of the analysis, in Model E at $I_t / I_c = 0.3$ the normal magnetic field component increases remarkably with turn gap decreasing. From this results, we assume that *the other turns effect* is enhanced with decreasing turn gap in Model E at $I_t / I_c = 0.3$, but it does not change with decreasing turn gap in other cases; on the other hand, *the canceling effect* is enhanced with decreasing turn gap in all cases. For these reasons, in model E at $I_t / I_c = 0.3$, the ac loss generation with decreasing turn gap does not change because of the competition of *the other turns effect* and *the canceling effect*; and in other case, the ac loss decrease with decreasing turn gap because of the domination of *the canceling effect*. However, in infinite solenoid coils (Model M) with null turn gap, we extrapolate that the ac loss does not disappear from the result of analyses. It is because there is another gap between the strands (strand gap) in the Roebel cables, and it distorts the magnetic field locally as well. At the ends of a coil generating high magnetic field where the magnetic field bends outward to generate the normal magnetic field component, the above-mentioned effect of the turn gap and the strand gap is not conspicuous: the primary factor

generating ac loss is not local magnetic field distortion, but the outward bend of the magnetic field in a coil.

C. Ac Loss Density Distribution in the Strand of Roebel Coils

The schematic figure of strands in Roebel cables in coils are shown in Fig. 5. In a coil, a strand adjoins with next turns of the Roebel cable. Figs 5(a-1) and (b-1) show strands in Model E. Figs 5(a-2) and (b-2) show strands in Model M.

The distribution along the strand length of the ac loss density for one-cycle of coil current is shown in Fig. 6; the ac loss energy which is averaged over the width of the strand is plotted along the strand axis for the half transposition length from the left end to the center in Fig. 2. The ac loss density distributions and the current lines on strands in the straight section and in the transposition section are shown in Figs. 7 and 8, respectively. Figs. 7(a) and 8(a) are for the Model E, and Figs. 7(b) and 8(b) are for the Model M, respectively, when the turn gap is 0.5mm. In each figure, the top shows ac loss energy distribution, and the bottom shows current lines.

At first, we look at the straight section of the strand marked A and B in Fig. 5(a). In Model M, the ac losses at A and B are almost same as shown in Figs. 6(a) and 6(b), because the strand adjoins the next turns both at A and B, and the normal magnetic field components generated by the strand current and the current in the next turn are canceled each other. Meanwhile, In Model E, the strand adjoins the next turn only at B; the ac losses in A is larger than those in B as shown in Figs. 6(a) and 6(b). At B, the ac losses in Models M and E agree with each other, apart from the case that the turn gap is 0.5 mm and $I_t / I_c = 0.3$ as shown in Fig. 6(a). Ac loss generation concentrates at the
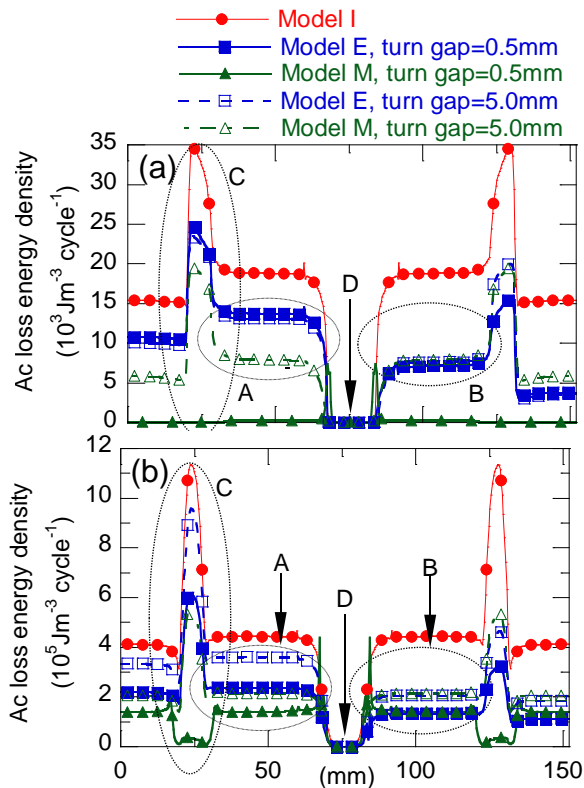
Fig. 6. Ac loss density distribution in longitudinal direction: (a) $I_t / I_c = 0.3$. (b) $I_t / I_c = 0.7$.
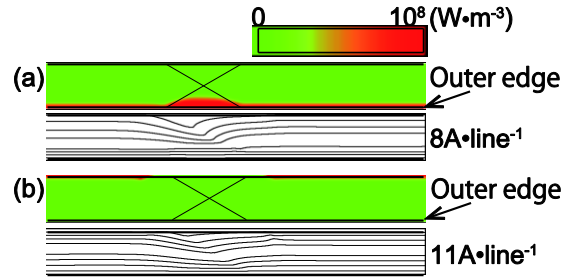

Fig. 7. The enlargement of the transposition section of other strands and is shown average ac loss density distribution for one cycle and current line at the peak of current, when the turn gap = 0.5 mm and $I_t / I_c = 0.7$. We show the other strands on ac loss density. (a) Model E, (b) Model M.
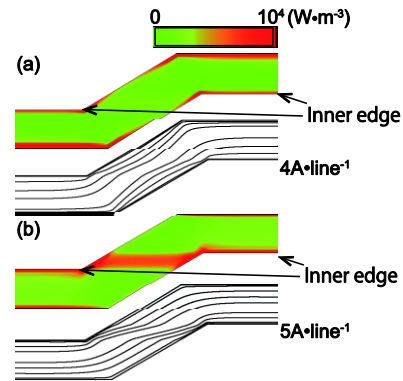

Fig. 8. The enlargement of the transposition section of the strand itself and this is shown average ac loss density distribution for one cycle and current line at the peak of the sine-wave current, when the turn gap = 0.5mm, $I_t/I_c = 0.3$: (a) Model E, (b) Model M.

outer edge in Model E in Fig. 7(a), whereas it concentrates at the inner edge in Model M in Fig. 7(b), because the turn gap (0.5mm) is smaller than the strand gap (2 mm). However, the generation of ac loss is much smaller at inner edge than at outer edge. From these results, we can assume that the wider gap is dominant for ac loss generation in Roebel coil, but the influence of the magnitude of ac loss generation at outer edge is superior to inner edge.

Secondary, we look at the transposition section of other strands marked C in Fig. 5(b). Larger ac loss is generated there than in the straight sections in Figs. 6(a) and 6(b), apart from the case that the turn gap is 0.5 mm in Model M and $I_t / I_c = 0.7$. Because the thickness of the cable is smaller (only two strands) at the outer edge in transposition section of other strands, large ac loss generation is observed there in Fig. 7(a). Meanwhile, when the turn gap is 0.5mm in Model M and $I_t/ I_c = 0.7$, the ac loss is smaller at the transposition section of other strands as shown in Fig. 6(b). In this case, the turn gaps are smaller than the strand gap, and the strand gap is the primary reason for the distortion of magnetic field. As shown in Fig. 7(b), more current flows near the inner edge of the strand, and ac loss generation concentrates near the inner edge rather than the outer edge at the straight section. Ac loss density at the inner edge is even smaller at the transposition section of other strands in Fig. 7(b).

At last, we look at the transposition section of the strand itself (D in Fig.5(a)). Ac loss is very small there in all cases as shown in Figs. 6(a) and 6(b). This is because the strands locate inside of the Roebel cable where the normal magnetic field component

is small. In Fig. 8, we can find quite different ac loss generations in Model M and Model E when the turn gap is 0.5 mm and current load ratio is 0.3: in Model M (Fig. 8(b)), ac loss generations are concentrated at the transposition section. When the turn gap is 0.5 mm in Model M, because the strand gap is larger than the turn gap, the current concentrates at the inner edge of a strand. This current must naturally flow across the strand width at the transposition section as shown in the bottom of Fig. 8(b). This might be the cause of the concentrated ac loss generation at the transposition section.

IV. SUMMARY

We have developed a novel model for electromagnetic field analyses of the Roebel cables wound into coil configurations. We used a thin-strip approximation in the model and considered the three-dimensional shapes of coated-conductor strands in coils wound with Roebel cables. We applied this model to three coils wound with Roebel cables to study their ac loss characteristics. We focused on the position in a coil (the coil end and the middle of the coil) and the gap between turns. Ac loss is more sensitive on the turn gap in the middle of coils. The turn gap as well as the gap between strands in a Roebel cable influences the distribution in ac loss generation in Roebel cables wound into coil configurations, and the wider of the turn gap and the strand gap dominates for ac loss generation.

REFERENCES

[1] W. Goldacker, A. Frank, A. Kudymow, R. Heller, A. Kling, S. terzieva, and C. Schmidt, "ROEBEL assembled coated conductors (RACC): Preparation, properties and progress," *IEEE Trans. Appl. Supercond.*, vol. 17, no. 2, pp. 3398-3401, Jun. 2007

[2] M. Nii, N. Amemiya, and T. Nakamura, "Three-dimensional model for numerical electromagnetic field analyses of coated superconductors and its application to Roebel cables," *Supercond. Sci. Technol.*, vol. 25, no. 9, p. 095011, 2012, (12pp).

[3] V. M. R. Zermeno, F. Frilli and F. Sirois, "A full 3D time-dependent electromagnetic model for Roebel cables," *Supercond. Sci. Technol.*, vol 26, no. 5, p. 052001, 2013, (8pp).

[4] E. Pardo and F. Frilli, "Numerical simulations of the angular dependence of magnetization AC losses: coated conductors, Roebel cables and double pancake coils," *Supercond. Sci. Technol.*, vol. 25, no. 1, p. 014008, 2012, (12pp).

[5] S. Terzieva, M. Vojenčiak, E. Pardo, F. Grilli, A. Drechsler, A. Kling, A. Kudymow, F. Gömöry and W. Goldacker, "Transport and magnetization ac losses of ROEBEL assembled coated conductor cables: measurements and calculations," *Supercond. Sci. Technol.*, vol. 23, no. 1, p. 014023, 2010, (8pp)

[6] Z. Jiang, M. Staines, R. A Badcock, N. J. Long, and N. Amemiya, "Transport AC loss measurement of a five strand YBCO Roebel cable," *Supercond. Sci. Technol.*, vol. 22, no. 9, p. 095002 (7pp).

[7] Z. Jiang, T. Komeda, N. Amemiya, N. J. long, M. Staines, R. A Badcock, C. Bumby and R. G. Buckley, "Total AC loss measurements in a six strand Roebel cable carrying an AC current in an AC magnetic field," *Supercond. Sci. Technol.*, vol. 26, no. 3, p. 035014, 2013, (10pp).

[8] N. Amemiya, T. Tsukamoto, M. Nii, T. Komeda, T. Nakamura and Z. Jiang, "Alternating current loss characteristics of a Roebel cable consisting of conductors and its three-dimensional structure," *Supercond. Sci. Technol.* accepted for publication.

[9] W. Goldacker, A. Frank, A. Kudymow, R. Heller, A. Kling, S. Trzieve, and C. Schmidt, "Status of high transport current ROEBEL assembled coated conductor cables," *Supercond. Sci. Technol.*, vol. 22, no. 3, p. 034003, 2009, (10pp).

[10] Z. Jiang, N. J. Long, R. A Badcock, M. Staines, R. A. Slade, A. D. Caplin and N. Amemiya, "AC loss measurements in pancake coils wound with 2G tapes and Roebel cable: dependence on spaceing between turns/strands," *Supercond. Sci. Technol.*, vol. 25, no. 3, p. 035002, 2012, (11pp).

[11] R. A Badcock, C. Bumby, Z. Jiang and N. J. Long, "Solenoid winding using YBCO Roebel cable," Superconductivity Centennial Conference 2011, Physics Procedia, vol. 36, pp. 1159-1164, 2012.

[12] Y. Ichiki and H. Ohsaki, "Numerical analysis of AC losses in YBCO coated conductor in external magnetic field," *Physica C*, vol. 412, pp.1015-1020, 2004.

[13] Y. B. Kim, C. F. Hempstead and A. R. Strnad, "Critical persistent currents in hard superconductors," *Phys. Rev. Lett*, vol. 9, no. 7, pp. 306-309, 1962.